Available online at www.sciencedirect.com
ScienceDirect
Physics Letters A 365 (2007) 278–283
PHYSICS LETTERS A
www.elsevier.com/locate/pla

Exponential convergence of a spectral projection of the KdV equation

Magnar Bjørkavåg, Henrik Kalisch *

Department of Mathematics, University of Bergen Johannes Bruns gate 12, 5008 Bergen, Norway

Received 22 September 2006; received in revised form 19 December 2006; accepted 20 December 2006

Available online 2 February 2007

Communicated by C.R. Doering

Abstract

It is shown that a spectral approximation of the Korteweg–de Vries equation converges exponentially fast to the true solution if the Fourier basis is used and if the solution is analytic in a fixed strip about the real axis. Computations are carried out which show that the exponential convergence rate can be achieved in practice.

Keywords: Spectral methods; Convergence rate; Solitary waves

1. Introduction

In this Letter, consideration is given to the convergence of a spectral projection of the periodic Korteweg–de Vries (KdV) equation

$$\partial_t u + u\partial_x u + \frac{1}{a^3}\partial_x^3 u = 0, \tag{1.1}$$

where a is a positive real number. Evidently, for the KdV equation on the line $\mathbb{R}$, a can be taken to be equal to 1, as it can be scaled out using the scaling $u(x,t) = \frac{1}{a}v(ax,t)$. However, as we are considering the equation on the interval $[0, 2\pi]$ with periodic boundary conditions, it will be convenient to leave a unspecified.

The KdV equation has been useful as a model equation in a variety of contexts, including the study of water waves, particle physics and flow in blood vessels [1–5], just to name a few. The discovery by Zabusky and Kruskal of the elastic interaction of solitary waves [6], and the subsequent formulation of a solution algorithm by way of solving an inverse-scattering problem [3,7], excited interest in the equation from both the mathematical and physical point of view. Along with the nonlinear Schrödinger equation, the KdV equation has become a paradigm for nonlinear wave equations featuring competing nonlinear and dispersive effects. Since the discovery by Cooley and Tukey of a fast algorithm to compute the discrete Fourier transform [8], spectral methods based on the fast Fourier transform have become a popular choice for the spatial discretization of nonlinear partial differential equations. In particular, in wave propagation problems, spectral projection has been widely used in connection with the Fourier basis.

The convergence of spectral projections of the KdV equation was proved by Maday and Quarteroni [9]. In particular, it was shown that if the solution $u(x,t)$ of (1.1) is smooth, then spectral convergence is achieved. That is, if u_N denotes the approximate solution with N grid points, then there is a constant λ_T, such that

$$\sup_{t\in[0,T]} \left\| u(\cdot,t) - u_N(\cdot,t) \right\| \leqslant \lambda_T N^{-m},$$

for any positive integer m. This estimate shows that the convergence rate is higher than any algebraic rate. It was announced in [10] that if the solution u is analytic in a strip about the real axis, then the convergence rate is in fact exponential. Thus there exist constants Λ_T and σ_T, depending on T, such that

$$\sup_{t\in[0,T]} \left\| u(\cdot,t) - u_N(\cdot,t) \right\| \leqslant \Lambda_T N e^{-\sigma_T N}. \tag{1.2}$$

In this Letter, a proof of this estimate will be given. Moreover, a numerical study will be conducted to show that this result is

* Corresponding author.
E-mail addresses: magnar.bjorkavag@math.uib.no (M. Bjørkavåg), henrik.kalisch@math.uib.no (H. Kalisch).

0375-9601/$ – see front matter
doi:10.1016/j.physleta.2006.12.085

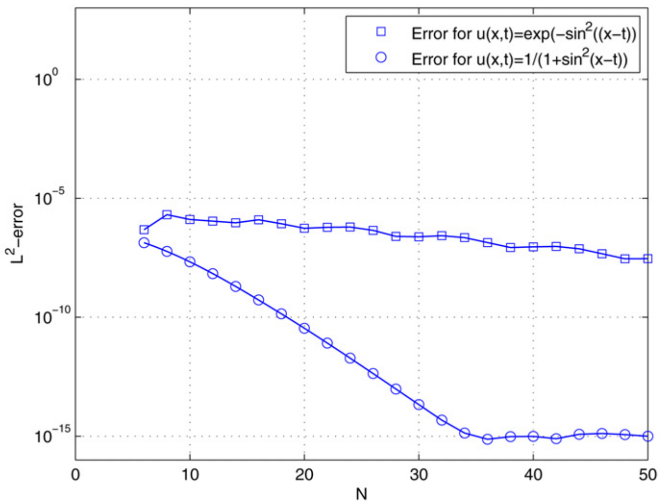

Fig. 1. It appears that the exponential convergence rate which holds for analytic solutions is more advantageous than the traditional spectral convergence which holds for smooth, but not analytic solutions.

indeed achievable in practice. To indicate the significance of the improvement, Fig. 1 shows the result of computing approximate solutions of the inhomogeneous equation

$$\partial_t u + u\partial_x u + \frac{1}{a^3}\partial_x^3 u = f.$$

First, the function $u(x,t) = e^{-\sin^2(x-t)}$ is used as the exact solution. Note that this function is smooth, but not analytic. The values shown as boxes in Fig. 1 are the L^2-error between the exact solution u and the computed approximation u_N. For this function, spectral convergence is achieved. Next, we use the function $u(x,t) = \frac{1}{1+\sin^2(x-t)}$ which is analytic. The resulting L^2-errors are shown as circles in Fig. 1, and it appears that the exponential convergence rate is by far superior to the spectral convergence rate. It should be noted that exponential convergence for spectral approximation schemes for evolution equations has been studied earlier. The exponential convergence of Galerkin schemes for parabolic equations has been previously advocated by Ferrari and Titi [11] and proved for the Ginsburg–Landau equation by Doelman, Jones, Margolin and Titi [12,13]. There have not been any previous results in this direction for dispersive equations like the KdV equation. However, Matthies and Scheel have used the analytic Gevrey norms to be defined in the next section in connection with dispersive equations in another context [14].

The plan of this Letter is as follows. In Section 2, we establish the relevant mathematical notation. In Section 3, the spectral approximation is defined, and the convergence estimate (1.2) is proved. Finally, in Section 4, numerical computations are shown to elucidate the result of Section 3. As it will turn out, the numerical observations match the theoretical predictions superbly.

2. Notation

The results in this Letter hold for solutions of (1.1) which are real-analytic functions of the spatial variable x. To quantify the domain of analyticity, we use the class of periodic analytic Gevrey spaces as introduced by Foias and Temam in [15]. For $\sigma > 0$, we define the Gevrey norm $\|\cdot\|_{G_\sigma}$ by

$$\|f\|_{G_\sigma}^2 = \sum_{k\in\mathbb{Z}} e^{2\sigma\sqrt{1+|k|^2}} \left|\hat{f}(k)\right|^2,$$

where the Fourier coefficients $\hat{f}(k)$ of the function f, periodic on the interval $[0, 2\pi]$ are defined by

$$\hat{f}(k) = \frac{1}{2\pi}\int_0^{2\pi} e^{-ikx} f(x)\,dx.$$

A Paley–Wiener type argument shows that functions in the space G_σ are analytic in a strip of width 2σ about the real axis. Similarly, the usual periodic Sobolev spaces are given by the norm

$$\|f\|_{H^s}^2 = \sum_{k\in\mathbb{Z}} \left(1+|k|^2\right)^s \left|\hat{f}(k)\right|^2.$$

In particular, for $s = 0$, the space $L^2(0, 2\pi)$ appears. For simplicity, the L^2-norm is written without any subscript, so that $\|f\| = \|f\|_{H^0}$. In the sequel, we will have occasion to use the inner product on this space, given by

$$(f, g) = \int_0^{2\pi} f(x)\overline{g(x)}\,dx.$$

Note also that for functions $f \in H^s$ with $s > \frac{1}{2}$, we have the Sobolev inequality, namely

$$\sup_x \left|f(x)\right| \leqslant C\|f\|_{H^s}$$

for some constant C.

3. Spectral projection

The spectral projection is achieved by solving a discrete set of ordinary differential equations in a finite-dimensional space. For this purpose, the subspace

$$S_N = \left\{e^{ikx} \mid k \in \mathbb{Z}, -N \leqslant k \leqslant N\right\}$$

of $L^2(0, 2\pi)$ is commonly used in connection with the Fourier basis. The self-adjoint operator P_N denotes the orthogonal projection from L^2 onto S_N, defined by

$$P_N f(x) = \sum_{-N\leqslant k\leqslant N} e^{ikx}\hat{f}(k).$$

Observe that P_N may also be characterized by the property that, for any $f \in L^2$, $P_N f$ is the unique element in S_N such that

$$(P_N f, \phi) = (f, \phi), \tag{3.1}$$

for all $\phi \in S_N$. Using a straightforward calculation, the following inequality can be proved [18]

$$\|f - P_N f\|_{H^r} \leqslant N^r e^{-\sigma N}\|f\|_{G_\sigma}, \tag{3.2}$$

for $r \geqslant 0$ and $\sigma > 0$. The Galerkin approximation to (1.1) is given by a function u_N from $[0,T]$ to S_N satisfying

$$\begin{cases} \left(\partial_t u_N + \frac{1}{2}\partial_x(u_N^2) + \frac{1}{a^3}\partial_x^3 u_N, \phi\right) = 0, & t \in [0,T], \\ u_N(0) = P_N u_0, \end{cases} \tag{3.3}$$

for all $\phi \in S_N$. Thus we assume that the solution is written as the sum

$$u_N(x,t) = \sum_{-N \leqslant k \leqslant N} \hat{u}_N(k,t) e^{ikx}.$$

The system (3.3) is a finite-dimensional system of ordinary differential equations. At present we are focusing attention on this semi-discrete system. The time integration of (3.3) is generally performed using some convenient time-discretization scheme, but we do not study any convergence results for such a scheme. With all notation and definitions in place, we can state the theorem advertised in the introduction.

Theorem 3.1. *Suppose $u(x,t)$ is a continuous function of t with values in the space G_σ for some $\sigma > 0$, and suppose that u solves (1.1). Given $T > 0$ and an integer $N > 0$, there exists a unique solution u_N of the finite-dimensional problem (3.3). Moreover, there is a constant Λ_T, such that*

$$\sup_{t \in [0,T]} \left\| u(\cdot,t) - u_N(\cdot,t) \right\| \leqslant \Lambda_T N e^{-\sigma N}.$$

One class of functions to which the theorem applies directly is the family of periodic traveling waves of the KdV equation. Note however that in general, even if initial data $u(x,0)$ are given in the periodic analytic Gevrey space G_σ, it cannot be concluded that the solution $u(x,t)$ is in G_σ at any other time $t > 0$. However, it can be shown that $u(x,t)$ is in G_{σ_t}, where σ_t is a decreasing function of t. In the case of the real line, algebraic dependence of σ_t on t has been recently proved [16].

In the proof of Theorem 3.1, it will be necessary to use some a priori bounds on Sobolev norms of the functions u and u_N. It is well known that the KdV equation has an infinite number of conserved integrals. As a consequence, it can be shown that all positive Sobolev norms of the solutions are bounded globally in time. Here, we only need the first three integer Sobolev norms.

Lemma 3.2. *Suppose u is a solution of (1.1). Then there are constants c_0, c_1 and c_2, such that*

$$\sup_{t \in [0,\infty)} \left\| u(\cdot,t) \right\| \leqslant c_0, \qquad \sup_{t \in [0,\infty)} \left\| u(\cdot,t) \right\|_{H^1} \leqslant c_1,$$
$$\sup_{t \in [0,\infty)} \left\| u(\cdot,t) \right\|_{H^2} \leqslant c_2.$$

For the spectral projection, it can also be shown that the first three integer Sobolev norms are bounded independently of N.

Lemma 3.3. *Suppose u_N is a solution of (3.3). Then there are constants c_0, c_1 and c_2, such that*

$$\sup_{t \in [0,T]} \left\| u_N(\cdot,t) \right\| \leqslant c_0, \qquad \sup_{t \in [0,T]} \left\| u_N(\cdot,t) \right\|_{H^1} \leqslant c_1,$$
$$\sup_{t \in [0,T]} \left\| u_N(\cdot,t) \right\|_{H^2} \leqslant c_2.$$

For a proof of these estimates, the reader is referred to [9,17].

Proof of Theorem 3.1. The existence of the solution u_N on the interval $[0,T]$ is proved by a combination of a fixed-point argument and the foregoing stability results. This is standard fare and will be omitted. To prove the convergence estimate, consider the function $h = P_N u - u_N \in S_N$ as the test function ϕ in the formula (3.3). Applying P_N to (1.1) and subtracting, there appears the equation

$$(\partial_t h, h) + \frac{1}{a^3}\left(\partial_x^3 h, h\right) + \frac{1}{2}\left(P_N \partial_x u^2 - \partial_x\left(u_N^2\right), h\right) = 0.$$

Since the third derivative operator is skew-symmetric, we have $(\partial_x^3 h, h) = 0$, so that the previous equation may be rewritten as

$$\frac{d}{dt}\|h\|^2 = \left(P_N\left(u^2\right) - u^2, h_x\right) + \left(u^2 - (P_N u)^2, h_x\right) + \left((P_N u)^2 - u_N^2, h_x\right). \tag{3.4}$$

Since P_N is the orthogonal projection onto S_N, (3.1) shows that the first term on the right in (3.4) is identically zero. The second term on the right can be treated as follows.

$$\begin{aligned} \left|\left(\partial_x\left(u^2 - (P_N u)^2\right), h\right)\right| &\leqslant \sup_x \left|\partial_x(u + P_N u)\right| \|u - P_N u\| \|h\| \\ &\quad + \sup_x |u + P_N u| \|u - P_N u\|_{H^1} \|h\| \\ &\leqslant 4C\|u\|_{H^2} N e^{-\sigma N} \|u\|_{G_\sigma} \|h\|. \end{aligned}$$

After an integration by parts, it appears that the third term on the right of (3.4) can be estimated by

$$\begin{aligned} \left|\left(\partial_x\left((P_N u)^2 - u_N^2\right), h\right)\right| &\leqslant \frac{1}{2} \sup_x \left|\partial_x(u_N + P_N u)\right| \|h\|^2 \\ &\leqslant \frac{C}{2} \|u_N + P_N u\|_{H^2} \|h\|^2. \end{aligned}$$

Hence it can be seen that the estimate

$$2\frac{d}{dt}\|h\| \leqslant 4C\|u\|_{H^2}\|u\|_{G_\sigma} N e^{-\sigma N} + \frac{C}{2}\left(\|u_N\|_{H^2} + \|u\|_{H^2}\right)\|h\|$$

appears. Letting $K = \sup_t \|u(\cdot,t)\|_{G_\sigma}$, this can be written as

$$\frac{d}{dt}\left\|h(\cdot,t)\right\| \leqslant 2Cc_2 K N e^{-\sigma N} + \frac{C}{2} c_2 \left\|h(\cdot,t)\right\|.$$

Now using Gronwall's inequality, we obtain

$$\left\|h(\cdot,t)\right\| \leqslant 2Cc_2 K N e^{-\sigma N} T e^{\frac{C}{2}c_2 T} + \left\|h(\cdot,0)\right\| e^{\frac{C}{2}c_2 T}.$$

Noting that $\|h(\cdot,0)\| = 0$, and using the triangle inequality and (3.2), we get the final estimate

$$\begin{aligned} \left\|u(\cdot,t) - u_N(\cdot,t)\right\| &\leqslant \left\|u(\cdot,t) - P_N u(\cdot,t)\right\| + \left\|h(\cdot,t)\right\| \\ &\leqslant \Lambda_T N e^{-\sigma N}, \end{aligned}$$

where $\Lambda_T = K + 2Cc_2 K T e^{\frac{C}{2}c_2 T}$. Taking the supremum over t concludes the proof. □

Table 1
Computations using a solitary wave with $c = 1$. Spectral convergence is apparent in the left half of the table, where the time step was $\Delta t = 10^{-6}$. Quadratic convergence is visible in the temporal discretization on the right, where $N = 8192$

N	L^2-error	Ratio	Δt	L^2-error	Ratio
36	1.19×10^{-6}		0.0625	5.97×10^{-3}	
72	1.13×10^{-6}	1.05	0.0312	1.51×10^{-3}	4.00
144	2.28×10^{-7}	4.95	0.0156	3.67×10^{-4}	3.99
288	1.59×10^{-9}	143.38	0.0078	9.18×10^{-5}	3.99
576	1.13×10^{-14}	140570.00	0.0039	2.29×10^{-5}	4.00
1152	4.75×10^{-15}	2.38	0.0020	5.73×10^{-6}	4.00

4. Numerical computations

In this section, some numerical computations will be presented with the aim of showing that the convergence rates proved in the previous section can actually be achieved in practical situations. Note that Theorem 3.1 applies in particular to the special case of a solitary wave $u(x,t) = \psi(x - ct)$ with translational velocity c. This is a solution of Eq. (1.1) if ψ has the special form

$$\psi(x) = 12\frac{\kappa^2}{a}\operatorname{sech}^2(\kappa a x),$$

for any $\kappa > 0$, and with velocity $c = 4\kappa^2$. Taking the Fourier transform of ψ yields

$$\hat{\psi}(k) = 6\pi k \operatorname{csch}\left(\frac{\pi k}{2\kappa a}\right),$$

revealing that ψ is in the space G_σ as long as $\sigma < \frac{\pi}{2\kappa a}$. Evidently, since the solution does not change its shape over time, it will continue to be in the space G_σ for all time, and Theorem 3.1 is applicable. It is now clear why the equation was written in the scaled form using the parameter a, because this allows us to put a solitary wave into the interval $[0, 2\pi]$ without it getting close to the boundary during the time evolution. With this scaling, the tails of the solitary wave are sufficiently small (below machine precision), so that periodic boundary conditions can be used to study the Cauchy problem on the line. The spectral projection of the KdV equation as described in the previous section is now coupled with a trapezoidal time-integration scheme. This scheme is implicit in the nonlinear term, so that an iteration has to be used at each time step. Since we generally took rather small time steps, only a few iterations were needed at each time step in order to achieve the convergence results shown in the following. In all computations shown $c = 1$ and $a = 34.2$ were used, corresponding to a value of σ slightly less than 0.0918. Computations were also performed for other values of c and a, and similar results obtain for these cases.

In the first three columns in Table 1, computations with a varying number of spatial gridpoints are shown. The third column in Table 1 represents the ratio between the errors in two consecutive calculations, and it can be seen that the spatial error decays rapidly with a rate that is apparently increasing. Also, the quadratic convergence of the time integration method can be seen in the fourth, fifth and sixth column of Table 1. As guided by the theory in the previous section, our main goal here will be to establish a relationship of the type

$$\sup_{t\in[0,T]} \left\| u(\cdot,t) - u_N(\cdot,t) \right\| \leqslant \Lambda N e^{-\sigma N},$$

where u is the solitary wave, and u_N is the spectral approximation. To this end, we seek the number σ by denoting the L^2-error

$$E = \sup_{t\in[0,T]} \left\| u(\cdot,t) - u_N(\cdot,t) \right\|,$$

and supposing a relation of the form

$$E = \Lambda N e^{-\sigma N}.$$

Now σ can be approximately computed by noting that we have the relation

$$\sigma = \frac{\log(E_1/E_2) - \log(N_1/N_2)}{N_2 - N_1}, \tag{4.1}$$

where E_1 and E_2 are the errors corresponding to two different computations with N_1 and N_2 gridpoints, respectively. Note that the constant Λ_T appearing in Theorem 3.1 is probably not sharp. In light of this, it is an added advantage that the constant Λ does not appear in (4.1).

Results of a few computations are listed in Tables 2, 3 and 4. These tables are for 1, 10 and 100 time steps, respectively. These tables show the error as well as the approximations for σ, and the deviation from the true value of σ. Note that we achieve a deviation of less than 15%. Here, a very small time step is taken, so that errors from the temporal discretization can be neglected. Corresponding graphs are shown in Figs. 2, 3 and 4. It is apparent that for longer time integrations, more grid points

Table 2
Numerical values for σ, and deviation from prediction after 1 time step. Results shown are for $c = 1$ and $a = 34.2$

N	L^2-error	σ	Deviation in %
76	1.1501×10^{-6}	0.0498	45.7
128	4.4699×10^{-7}	0.0625	31.9
180	1.1289×10^{-7}	0.0695	24.3
232	2.2602×10^{-8}	0.0738	19.7
284	3.9179×10^{-9}	0.0766	16.5
336	6.1547×10^{-10}	0.0787	14.3
388	8.9993×10^{-11}	0.0803	12.5
440	1.2458×10^{-11}	0.0816	11.2

Table 3
Numerical values for σ, and deviation from prediction after 10 time steps. Results shown are for $c = 1$ and $a = 34.2$

N	L^2-error	σ	Deviation in %
76	1.1501×10^{-5}	0.0498	45.7
128	4.4699×10^{-6}	0.0625	31.9
180	1.1289×10^{-6}	0.0695	24.3
232	2.2602×10^{-7}	0.0738	19.7
284	3.9179×10^{-8}	0.0766	16.5
336	6.1547×10^{-9}	0.0787	14.3
388	8.9993×10^{-10}	0.0803	12.5
440	1.2459×10^{-10}	0.0815	11.2

Table 4
Numerical values for σ, and deviation from prediction after 100 time steps. Results shown are for $c = 1$ and $a = 34.2$

N	L^2-error	σ	Deviation in %
76	1.1501×10^{-4}	0.0498	45.7
128	4.4699×10^{-5}	0.0625	31.9
180	1.1289×10^{-5}	0.0695	24.3
232	2.2602×10^{-6}	0.0738	19.7
284	3.9179×10^{-7}	0.0766	16.5
336	6.1547×10^{-8}	0.0787	14.3
388	8.9993×10^{-9}	0.0803	12.5
440	1.2458×10^{-9}	0.0815	11.2

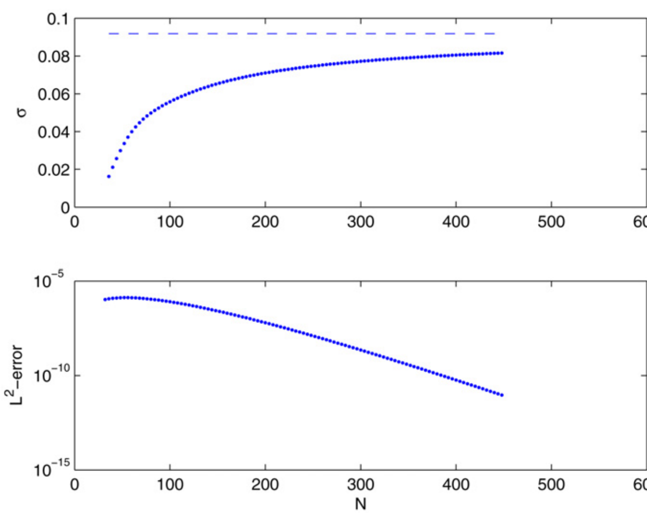

Fig. 2. Error and approximation of σ after 1 time step. The dashed line represents the theoretical value of σ. Results shown are for $c = 1$ and $a = 34.2$.

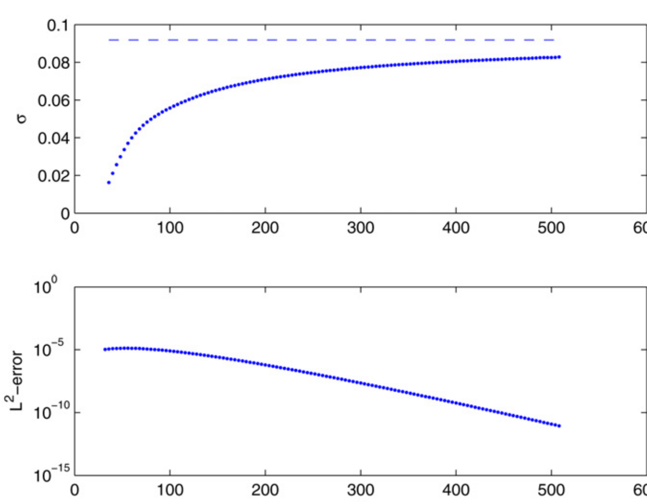

Fig. 3. Error and approximation of σ after 10 time steps. The dashed line represents the theoretical value of σ. Results shown are for $c = 1$ and $a = 34.2$.

are required to achieve the same error. This is the reason why the graph in Fig. 2 appears shorter than in Figs. 3 and 4. In all three cases, the L^2-error approaches machine precision before the approximations reach the asymptotic convergence rate. Therefore, to improve the approximation of σ, a least-squares

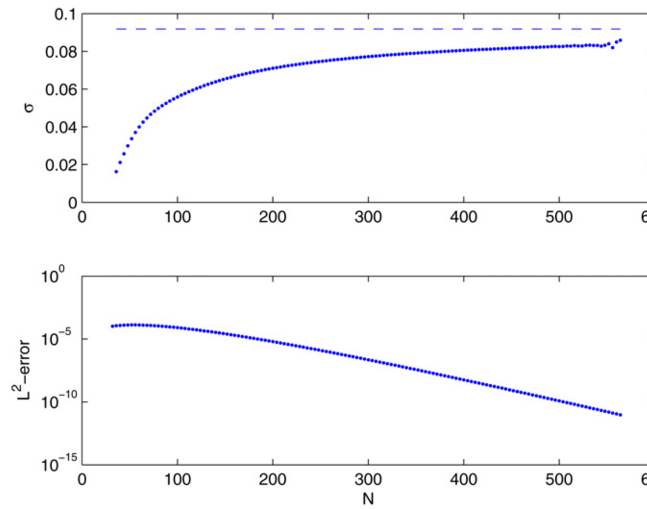

Fig. 4. Error and approximation of σ after 100 time steps. The dashed line represents the theoretical value of σ. Results shown are for $c = 1$ and $a = 34.2$.

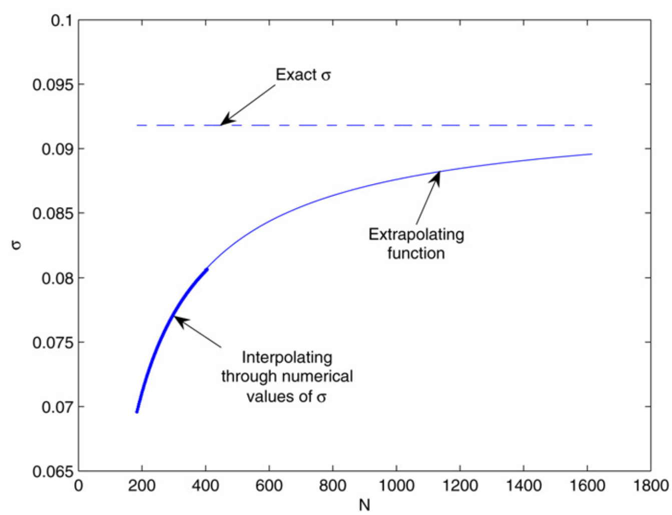

Fig. 5. Approximation of σ, extrapolated by least-squares fit using the function $\sigma = \frac{N}{a+bN}$. The dashed line represents the exact value $\sigma \sim 0.0918$. The asymptote of the extrapolating function is $1/b = 0.093$.

fit is made over all values of σ computed. For the data fit, the form

$$\sigma = \frac{N}{a + bN}$$

is assumed. The fitted curve is shown in Fig. 5. It appears that the computed value of σ found from the extrapolation approaches the theoretical value asymptotically. Indeed we find that $1/b = 0.093$, while $\sigma \sim 0.0918$.

In conclusion, it can be said that the theoretical convergence result of Theorem 3.1 can be achieved without much difficulty in practical computations. The implications of this are twofold. On the one hand, rapid convergence like the one exhibited in (1.2) point towards the use of simple models such as the KdV equation in order to capture the essence of a physical situation. On the other hand, the pursuit of similar convergence estimates for more complicated models retaining more refined physical features could prove to be a fruitful endeavor if one knows that such strong results can be proved in the model case.

Acknowledgements

This research was supported in part by the Research Council of Norway.

References

[1] J. Boussinesq, J. Math. Pures Appl. 17 (1872) 55.
[2] R.C. Cascaval, Variable coefficient KdV equations and waves in elastic tubes, in: Evolution Equations, in: Lecture Notes in Pure and Applied Mathematics, vol. 234, Dekker, New York, 2003, pp. 57–69.
[3] P.G. Drazin, R.S. Johnson, Solitons: An Introduction, Cambridge Texts in Applied Mathematics, Cambridge Univ. Press, Cambridge, 1989.
[4] A. Jeffrey, T. Kakutani, SIAM Rev. 14 (1972) 582.
[5] D.J. Korteweg, G. de Vries, Philos. Mag. 39 (1895) 422.
[6] N.J. Zabusky, M.D. Kruskal, Phys. Rev. Lett. 15 (1965) 240.
[7] R. Beals, P. Deift, C. Tomei, Direct and Inverse Scattering on the Line, Mathematical Surveys and Monographs, vol. 28, American Mathematical Society, Providence, RI, 1988.
[8] J.M. Cooley, J.W. Tukey, Math. Comp. 19 (1965) 297.
[9] Y. Maday, A. Quarteroni, RAIRO Modél. Math. Anal. Numér. 22 (1988) 499.
[10] H. Kalisch, C. R. Math. 341 (2005) 457.
[11] A.B. Ferrari, E.S. Titi, Comm. Partial Differential Equations 23 (1998) 1.
[12] A. Doelman, E.S. Titi, Numer. Funct. Anal. Optim. 14 (1993) 299.
[13] D.A. Jones, L.G. Margolin, E.S. Titi, Theor. Comput. Fluid Mechanics 7 (1995) 243.
[14] K. Matthies, A. Scheel, Trans. Am. Math. Soc. 355 (2003) 747.
[15] C. Foias, R. Temam, J. Functional Anal. 87 (1989) 359.
[16] J.L. Bona, Z. Grujić, H. Kalisch, Annu. Inst. H. Poincaré, Anal. Non-Linéaire 22 (2005) 783.
[17] R. Temam, J. Math. Pures Appl. 48 (1969) 159.
[18] C. Canuto, M.Y. Hussaini, A. Quarteroni, T.A. Zang, Spectral Methods in Fluid Dynamics, Springer, 1988.